A "Core−Shell" Approach to Producing 3D Polymer Nanocomposites

Olga Kalinina and Eugenia Kumacheva*

Department of Chemistry, University of Toronto, Toronto, Ontario, M5S 3H6 Canada

Received October 9, 1998; Revised Manuscript Received March 11, 1999

ABSTRACT: A new strategy to producing three-dimensional (3D) ordered polymer nanocomposites is proposed that employs a core−shell latex morphology. We synthesized core−shell latex particles in which a core-forming polymer had a glass transition temperature significantly higher than that of a shell-forming polymer. Particles were assembled in a 3D close-packed structure and annealed in such a way that latex cores remained intact while latex shells deformed and flew. As a result, a continuous matrix was formed that contained an organized 3D array of monodisperse "core" particles. A possibility to control the functionality of the "core" beads was demonstrated by labeling the core-forming polymer with a fluorescent dye. We discuss conditions in which an ordered, void-free polymer nanocomposite can be obtained.

Introduction

Latex particles with dimensions varying from tens of nanometers to a few microns have potential applications in electro- and nonlinear optics, optical and magnetic data storage, and chemical and biochemical sensors. High monodispersity and easy functionalization of latex microspheres along with their ability under particular conditions to form two-dimensional (2D) or three-dimensional (3D) ordered arrays make them attractive objects for material science.[1−6]

A challenging task is to preserve these advantages upon incorporation of latex particles in various matrices, e.g., in polymer blends. However, simple mixing of latexes does not provide a regular interparticle distance.[7,8] In addition, upon annealing at elevated temperatures particles collide and coarsen due coalescence and/or Ostwald ripening.[9] As a result, after a certain period, particle size distribution becomes far from monodisperse. To suppress microsphere collisions that originate from the Brownian motion and flow of the intervening polymer from narrow to wide gaps between particles, two requirements have to be fulfilled. First, a matrix polymer should act as an elastic barrier to prevent particle coalescence. Second, a uniform distribution in the interparticle distance should be maintained to eliminate pressure gradients in the system upon annealing. While the first condition can be realized by using suitable matrix-forming polymers, the second demand needs nontrivial approaches.

One of the strategies that has been developed in recent years is based on a spontaneous assembly of latex particles in liquid colloid crystals. In these systems, crystallization is driven by a proper balance of attraction and repulsion forces acting between the particles. The liquid colloid crystals are then solidified either by liquid-phase chemical reactions of inorganic materials added to the dispersion[1] or by polymerization of monomers introduced into the liquid phase.[3,10]

In this article, we describe an alternative approach to producing organized submicron polymeric structures that employs core−shell latex particles with a hard functionalized core and a soft inert shell. In contrast, previous attempts to employ core−shell latex particles with glassy cores and soft shells were aimed mainly at prevention of core aggregation and resulted in partial exclusion of the shell polymer from the gap between cores.[8]

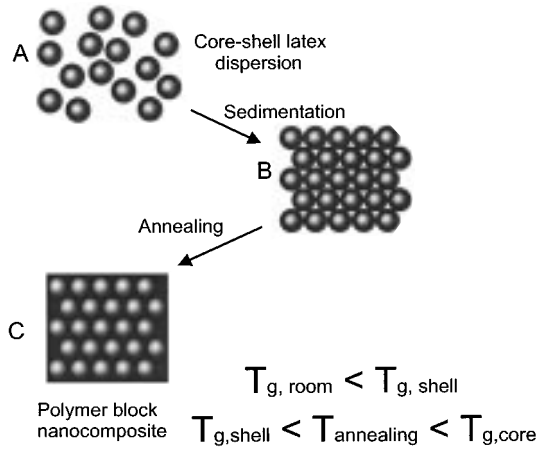

Figure 1. Illustration of the proposed approach to the formation of a 3D polymer nanocomposite material. Stage A: synthesis of the core−shell latex particles with hard functionalized cores and soft inert shells. Stage B: assembly of latex particles in a 3D close-packed structure. Stage C: heat treatment of the 3D compact that leads to flow of soft shells and formation of a nanocomposite polymer.

We describe the synthesis of functionalized core−shell latex particles, discuss the conditions required for the preparation of polymer nanocomposites, examine the morphology of the material, and review possible applications of the proposed approach. Although both thin films and block polymer materials can be prepared by the proposed method, this work was aimed at the formation of a three-dimensional polymeric nanocomposite.

Concept of Formation of 3D Ordered Polymer Structure. Figure 1 demonstrates the concept of the proposed approach. Stage A involves the synthesis of the core−shell latex particles that consist of a hard core and a somewhat softer shell. The monomers chosen for the synthesis of the core and shell polymers must satisfy two important requirements. First, the glass transition temperature (T_g) of the core-forming polymer (CFP) and the shell-forming polymer (SFP) should be such that that upon annealing the SFP softens and flows while the CFP remains intact. Second, the shell-forming

10.1021/ma981583o CCC: $18.00
Published on Web 05/18/1999

Scheme 1

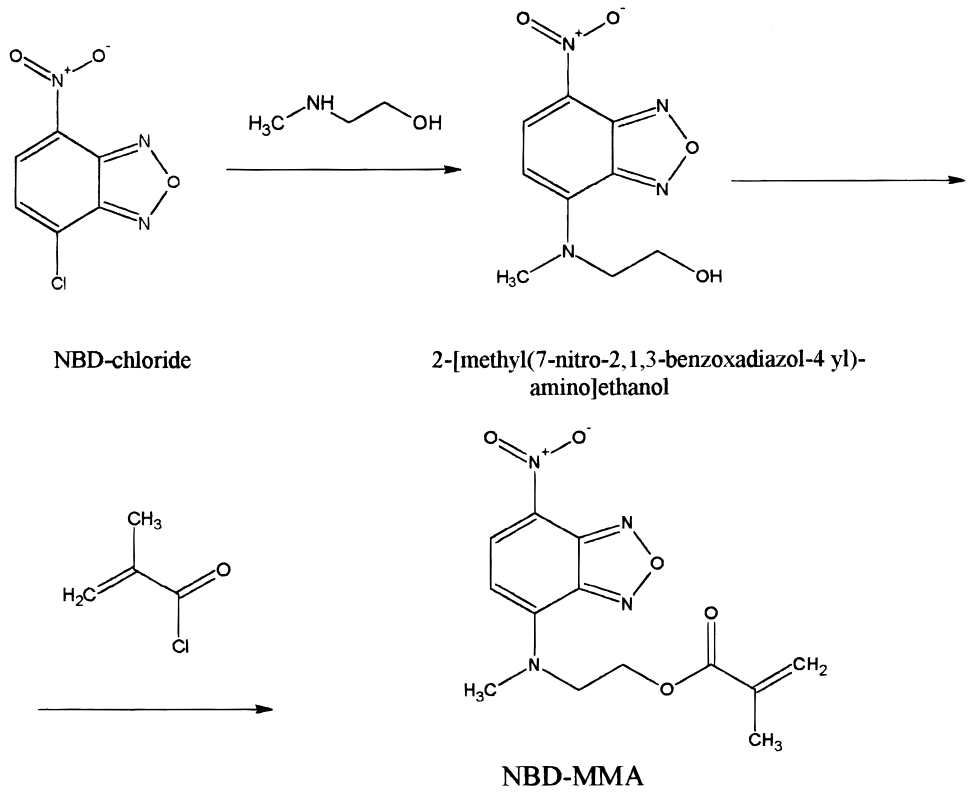

polymer must have a T_g well above the room temperature. At stage A, various functional groups can be attached to the CFP or to the SFP. To suppress any possible diffusion of functionalized macrochains between the core and the shell during synthesis or during annealing, the core polymer is cross-linked. At stage B, the particles settle and come in contact. Fabrication of the composite polymer material is completed by annealing of the dry compact (stage C). At this stage, the system is heated above the T_g of the SFP. The shell-forming polymer flows filling voids between particles and ultimately forms a continuous transparent matrix. Intact "core" beads form an ordered array in the SFP.

The proposed strategy for preparing ordered arrays of functional polymeric spheres in a uniform polymeric matrix provides several levels of control of the structure and function of the nanocomposite. First, the diameters of the cores and the thicknesses of the shells can be varied and controlled leading to the variation in particle number density in the nanocomposite material. Second, the functionality of the cores can be manipulated through the use of appropriate functional comonomers. Third, the composition of the shells can be controlled by judicious choice of comonomers.

Few considerations have to be taken in account. First, to eliminate pressure gradients in the system during annealing, the "core" particles have to be monodisperse and the shells have to be uniform in thickness. Second, the shells have to be sufficiently thick that upon annealing the SFP fills the interstitial spaces between the "core" particles. Third, the composition of the SFP should be such that the shells possess enough elasticity to act as a barrier to prevent the collisions of cores.

Experimental Section

Materials. Methyl methacrylate (MMA, 99%) and butyl methacrylate (BMA, 99%) monomers were purchased from Fluka and purified by distillation under reduced pressure. Ethylene glycole dimethacrylate (EGDMA, Aldrich, 98%) was used as supplied. The water was purified by double distillation and deionized using Millipore Milli-Q Plus purification systems (Millipore Corporation). The ionic initiator, potassium persulfate (Aldrich, 99%), the nonionic initiator 2,2′-azobis(2-methylpropionitrile) (AIBN, Kodak, 99%), and the chain-transfer agent dodecylmercaptan (DDM, Aldrich, 98%) were used as received.

A fluorescent dye-labeled comonomer 4-amino-7-nitrobenzo-2-oxa-1,3-diazole−MMA (NBD−MMA) was synthesized in two steps. 4-Chloro-7-nitro-2,1,3-benzooxadiazole (NBD−chloride, Aldrich, 98%) with an excess of 2-(methylamino)ethanol (Aldrich, 99%) in ethanol was refluxed for 2 h, then kept upon stirring overnight, and filtered. The resulting 2-[methyl-(7-nitro-2,1,3-benzoxadiazol-4-yl) amino]ethanol was purified by recrystallization from ethanol and characterized by ^{1}H NMR (^{1}H NMR ($CDCl_3$): 8.45 (1H), 6.20 (1H), 4.60 (1H), 3.50 (3H), 4.60 (2H), 4.30 (2H)). The second step included coupling of the cooled product with an excess of methachroyloyl chloride (Aldrich, 90%) in the presence of triethylamine in dry tetrahydrofuran (THF). Following ca. 12 h stirring, the solution was neutralized by adding aqueous sodium hydroxide, washed with water, and dried over anhydrous sodium sulfate. After removing the solvent, the resulting 2-[methyl-(7-nitro-2,1,3-benzooxadiazol-4-ylamino]ethyl 2-methyl methacrylate (NBD−MMA) was purified on silica gel column with cyclohexane: acetone (1:1) as eluent. ^{1}H NMR ($CDCl_3$): 8.40 (1H), 6.20 (1H), 5.90 (1H), 5.50 (1H), 4.50 (4H), 3.45 (3H), 1.90 (3H). The synthesis of NBD−MMA is shown in Scheme 1.

Latex Synthesis. Core−shell latexes described in this work were synthesized via two- or three-stage polymerization using a semicontinuous reaction scheme. All reactions were carried out in a three-neck flask at 80 ± 0.1 °C equipped with a condenser, mechanical stirrer, and inlets for nitrogen and monomer. Prior to polymerization, the reaction mixture was purged with nitrogen, and a small positive pressure of nitrogen was maintained during the synthesis.

Stage 1. At the stage of seeding, water, potassium persulfate, and a small amount of MMA (in most cases ~10% of the total monomer weight) were precharged into the reaction vessel,

heated, and stirred for 1 h. The rest of the monomer with a small amount of dodecylmercaptan was fed to the reactor via a fluid metering pump at a constant rate. The pumping time was usually 3−4 h. It was assumed that the reaction was carried out in a starve-fed regime. When the addition of the monomer was complete, the reaction was continued for an additional 1 h.

Stage 2. About 10 mL of the latex dispersion from the previous step, water, and AIBN were mixed in the reactor vessel. A monomer solution was then pumped into the flask at the rate 0.01−0.05 mL/min under constant stirring. EGDMA used as a cross-linking agent, and a fluorescent comonomer NBD−MMA were added to the reaction mixture during the synthesis of cores.

Stage 3. The synthesis of the MMA−BMA copolymer shells to the PMMA cores was carried out similarly to the synthesis of cores at stage 2. A mixture of MMA and BMA at the weight ratio 2:1 was added to the reactor.

The synthesis of the core−shell particles with the total diameter not exceeding ca. 500 nm was accomplished in two stages similar to stage 1 and stage 3.

Latex Characterization. The concentration of latex dispersions was determined gravimetrically. The gel fraction of the CFP was determined by measuring the fraction of the dissolved polymer in THF.

The dimensions and size distribution of particles smaller than 350 nm were measured by quasi-elastic light scattering (Brookhaven BI-90). The dimensions of larger particles were analyzed by scanning electron microscopy (SEM) on a Hitachi S-570 scanning electron microscope at an accelerating voltage of 15 kV. The working distance was 15 mm. A drop of a diluted (<0.5 wt %) latex dispersion was dried on the aluminum stub and then coated with gold.

The glass transition temperatures of the CFP and the SFP were examined on a Perkin-Elmer DSC-7 differential scanning calorimeter under a N_2 atmosphere at a heating rate of 5 °C/min.

Preparation of Polymer Films. To produce films with a thickness not exceeding ca. 200 μm, latex dispersions were cast on various substrates (including glass, Teflon, "bare mica", and hydrophobized mica) and allowed to dry. To obtain a 3D polymer nanocomposite, latex dispersions were poured into cylindrical containers with a detachable flat bottom. The containers were covered to suppress water evaporation, and the particles were allowed to settle. After particle sedimentation was completed, the clear supernatant liquid was carefully removed from a cylinder, and the remaining water was allowed to evaporate. The dry compact of latex particles was annealed at 110 °C for a time period, the range of which depended on the sample thickness (usually from 1 to 16 h).

Studies of Film Morphology. The surface structure of the polymer material was examined by SEM and by atomic force microscopy (AFM) in the contact mode using a Nanoscope III microscope (Digital Instruments, Santa Barbara, CA). AFM imaging was performed under ambient conditions. The spring constant was 0.38 N/m. The scan rates varied in the range from 1 to 4 Hz.

The surface and the bulk morphology of the polymer nanocomposite were studied by laser confocal fluorescent microscopy (LCFM) on a Bio-Rad MRC 600 microscope. The 488 nm line of the Ar ion laser was employed for the excitation of the NBD dye. The vertical and the lateral resolutions were 0.3 and 0.7 μm, respectively.

The SEM and LCFM images were analyzed using Image Tools software (University of Texas, Health Science Centre).

Results and Discussions

Latex Synthesis. In the approach discussed above, the compositions and the dimensions of the latex cores and the latex shells play an important role in the design and morphology of the nanocomposite polymer material. The criteria for the selection of recipes for latex synthesis include the dimensions of cores and shells, particle monodispersity, dispersion stability, and the absence of secondary seeding. In addition, the relationship between the glass transition temperatures of the CFP and the SFP has to fulfill the requirement specified in the description of the approach.

In the material described in this work, the latex cores consisted of poly(methyl methacrylate) and the latex shells were composed of a methyl methacrylate−butyl methacrylate copolymer. We were unable to synthesize latex particles with dimensions larger than ca. 200 nm, using an ionic surfactant sodium dodecyl sulfate (SDS) in the emulsion polymerization. These attempts resulted in a massive seeding of small secondary particles. On the other hand, a surfactant-free synthesis led to latex coagulation. To overcome these problems, we modified the approach originally developed by Rudin et al.[11] First, the synthesis of the core−shell particles with a diameter larger than ca. 500 nm was carried out by a seeded semicontinuous emulsion polymerization accomplished in sequential stages; i.e., at each successive stage latex

Table 1. Recipe for the Three-Stage Emulsion Polymerization of the 1050 nm Core−Shell Latex Particles

	stage 1	stage 2	stage 3
precharge			
deionized water, g	70	70	40
seeds from previous step, g		20	20
potassium persulfate, g	0.2		
AIBN, g		0.005	0.005
pumping mixture			
MMA, g	30	7	4
BMA, g			2
DDM, g	0.088	0.052	0.276
EGDMA, g	1.068	0.032	
NBD−MMA, g	0.01	0.0035	
AIBN, g		0.052	0.396
ionic initiator solution added simultaneously with the monomer mixture			
potassium persulfate, g			0.0026
water, g			2.6
particle size, nm	500	640	1050

Table 2. Recipe for the Two-Stage Synthesis of the 560 nm Core−Shell Latex Particles

	stage 1	stage 2
precharge		
MMA, g	3	70
deionized water, g	70	20
seeds from previous step, g		
potassium persulfate, g	0.2	0.005
AIBN, g		
pumping mixture 1[a]		7
MMA (g)	15	
BMA (g)		0.052
DDM (g)	0.06	0.032
EGDMA (g)	0.6	0.0035
NBD−MMA (g)	0.007	0.052
AIBN (g)		
pumping mixture 2[a]		
MMA (g)	8	
BMA (g)	4	
DDM (g)	0.044	
particle size (nm)		
following an addition of mixture 1	370	
following an addition of mixture 2	500	
at the end of synthesis		560

[a] Since the average particle size that can be achieved at the first stage of synthesis without coagulation is ca. 500 nm, the synthesis of latex shells was started at the first stage by inducing mixture 1 for the synthesis of cores and mixture 2 for the synthesis of shells.

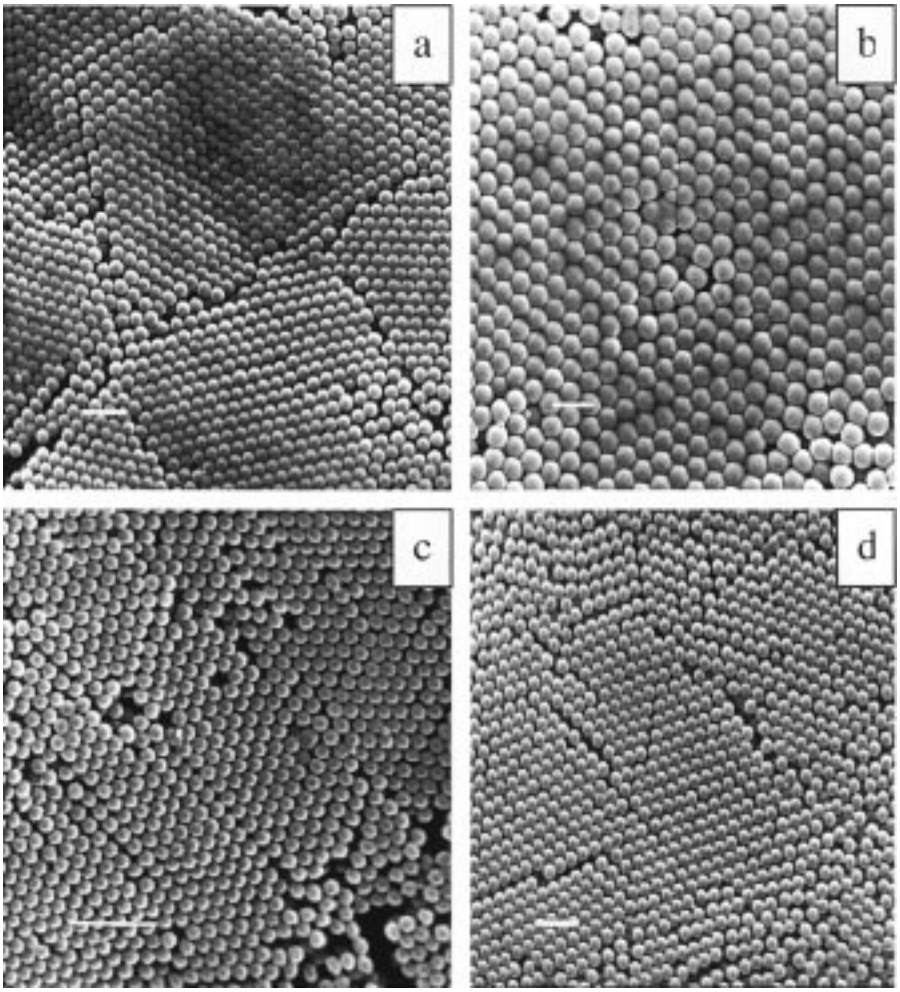

Figure 2. Scanning electron microscopy images of latex particles synthesized (a, b) using the recipe given in Table 1, and (c, d) using the recipe given in Table 2: (a) "core" particles after stage 2, (b) core−shell particles after stage 3, (c) "core" particles after stage 1, and (d) core−shell particles after stage 2. Scale bar is 2 μm.

particles from the previous stage were used as seeds. Second, a mixed-initiator approach, i.e., a combination of the oil-soluble and water-soluble initiators, at different stages of synthesis was used to provide polymerization in the bulk of latex particles and their stabilization. According to Rudin,[11] low-molecular weight oligomer-containing residues of an ionic initiator potassium persulfate play the role of an in situ surfactant in the system.

Preparation of the Latex Cores. The high-T_g latex cores containing a fluorescent dye substituent were synthesized in one or two stages, depending on the size of the core particles desired. In the first stage, particles with the diameter not exceeding ~500 nm were synthesized in a semibatch mode using water-soluble initiator potassium persulfate. To obtain larger particles, a second stage polymerization was carried out under monomer-starved conditions. The dispersion obtained in the first stage was diluted to reduce particle number density, and an oil-soluble initiator (AIBN) was used to suppress secondary seeding and to provide polymerization in the bulk of growing particles. At this stage, the amount of the in-situ surfactant was still sufficient to provide the stability of dispersion.

The cross-linking agent (ethylene glycol dimethacrylate) was added to the system at the maximum concentration 2 mol % which provided ~80% gel fraction in the CFP. A larger amount of the cross-linking agent led to latex aggregation.

The fluorescent dye was introduced in the CFP through the use of a methacrylate comonomer containing dye 4-amino-7-nitrobenzo-2-oxa-1,3-diazole (NBD). Winnik et al.[12] have shown that NBD-methacrylate is uniformly and randomly distributed along the PMMA chain when copolymerized in small amounts with MMA. The concentration of the NBD-labeled monomer in the reaction mixture was determined by the fluorescent intensity required to visualize the "core" particles in the bulk material by LCFM.

Growth of the Latex Shells. The lower T_g inert shells were grown onto the surface of the "core" particles in the last stage of the synthesis. Latex particles from the previous stage were used as seeds, and a mixture of BMA and MMA was induced into the reaction vessel. The weight ratio of BMA/MMA in the mixture was chosen to obtain the target glass transition temperature of the SFP (see below). Since the amount of the in-situ surfactant in the system was not enough to suppress particle coagulation at this stage, an ionic initiator potassium persulfate was added to the reaction mixture.

The variation in the average size of the particles could be achieved by changing the recipes or the number of stages. For example, core−shell particles with the average diameter 1050 nm were synthesized in three stages, while smaller particles with the dimensions 560 nm were obtained in two stages. The recipes for the synthesis of these dispersions are given in Tables 2 and 3.

Table 3. Volume Fraction of the CFP in the Polymer Nanocomposite Formed from Core−Shell Particles with the Different Core Diameter and Shell Thickness

$l_s =$	r_c, μm								
$r_p - r_c$, μm	0.15	0.20	0.25	0.30	0.35	0.40	0.45	0.50	0.60
0.025	42	52	*58*	*63*	*67*	*70*	*73*	*75*	*79*
0.050	22	30	36	42	47	51	55	*58*	*63*
0.075	12	19	24	30	34	38	42	46	51
0.100	8	12	17	22	26	30	33	36	42
0.125	5	9	12	16	20	23	26	30	35
0.150	4	6	9	13	16	19	22	24	30
0.175	3	5	7	10	12	15	18	20	25
0.20	2	4	6	8	10	12	15	17	22
0.25	1	2	4	5	7	9	10	11	18

Figure 2 displays the SEM images of latex microspheres with different dimensions obtained at different stages of synthesis. The diameters of cores and the thicknesses of shells were obtained by measuring microsphere sizes after each stage of synthesis. In Figure 2a the average core diameter is 640 nm, while the mean diameter of the core−shell particles shown in Figure 2b is 1050 nm. Consequently, the thickness of the latex shell is ca. 205 nm. Correspondingly, for smaller core−shell particles shown in Figure 2c,d, the average diameter of cores is 370 nm, the diameter of the core−shell particles is 560 nm, and the shell thickness is ca. 95 nm. The polydispersity index for both latex cores and core−shell particles did not exceed 0.03.

Glass Transition Temperatures of the CFP and the SFP. The difference in the glass transition temperatures of the latex cores and the latex shells is a crucial point of the suggested approach: at the temperature of annealing the CFP remains intact, whereas the shell polymer flows and fills in the gaps between microspheres. Thus, the lower limit of the processing temperature is bounded by the T_g of the SFP, and its higher limit is controlled by the T_g of the CFP.

The dependence of the T_g of the CFP and the SFP as a function of their composition is demonstrated in Figure 3. The variation of the T_g of the CFP with the increase of the amount of the cross-linking agent is shown in Figure 3a. The value of 134 °C is achieved at the concentration of EGDMA in the reaction mixture of 2 mol % (the maximum concentration of EGDMA that did not cause latex coagulation). Figure 3b demonstrates the change in the T_g of the SFP with the increase of BMA in the shell polymer. A copolymerization of MMA and BMA allowed to provide a wide range of the glass transition temperatures ranging from 36 °C (pure PBMA) to 124 °C (PMMA). Assuming that the operation temperature of the polymer block material is ca. 70 °C, we determined the lower limit of the T_g of the SFP to be 90 °C. This value of T_g was achieved at 30 wt % concentration of the BMA in the SFP. The temperature of film formation was 110 °C, i.e., about 20 °C higher than the T_g of the SFP.

Geometric Considerations on the Ratio of Core and Shell Dimensions. The suggested approach may lead to various types of morphologies of the ultimate polymer composite: from the rigid beads just "glued" together by the shell-forming polymer in a manner similar to sintering of silica particles[13] to a composite material in which molten shells form a continuous matrix. Here, our work was focused on the second type of morphology.

Generally, latex films are formed through a transformation of close-packed latex microspheres to polyhedra

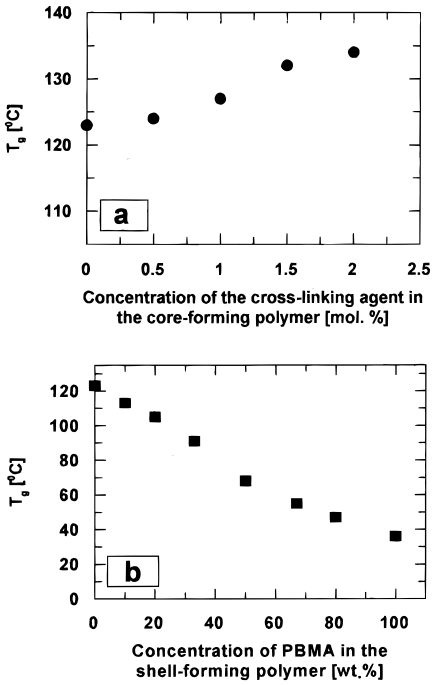

Figure 3. Variation of the glass transition temperatures of the core-forming and the shell-forming polymers: (a) T_g of the CFP as a function of the concentration of the cross-linking agent EGDMA; (b) T_g of the SFP as a function of the concentration of PBMA.

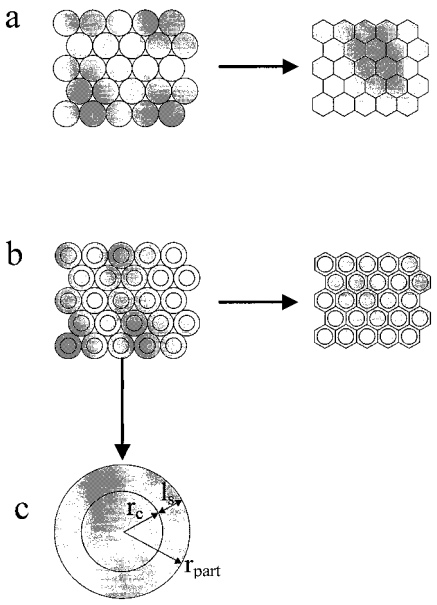

Figure 4. Scheme of particle deformation upon film formation: (a) deformation of homogeneous latex particles; (b) deformation of core−shell particles in the proposed approach; (c) scheme of a core−shell particle.

filling interstitial spaces (Figure 4a). In contrast, in the proposed approach this transformation should be provided by the deformation and flow of soft shells only. Therefore, the ratio between the core radius (r_c) and the shell thickness (l_s) should be maintained such that the volume of the SFP is sufficient to fill gaps between the cores (Figure 4b).

When latex particles come in contact, the packing fraction is

$$\phi = V_{part.}/(V_{part.} + V_{void}) \quad (1)$$

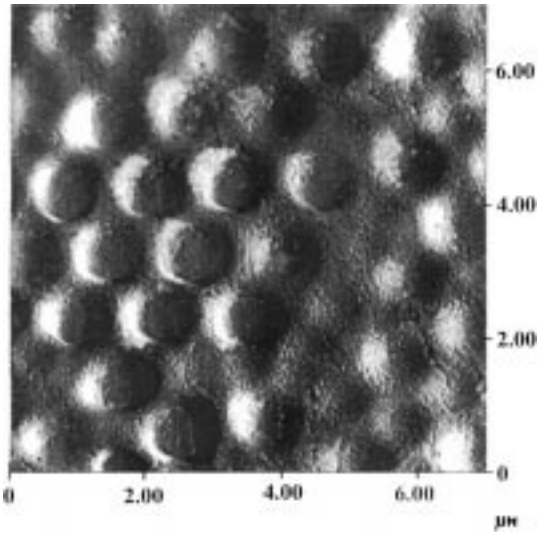

Figure 5. AFM image of the surface of the polymer nanocomposite formed from core−shell latex particles synthesized using the recipe given in Table 1.

where $V_{part.}$ is the volume of spherical particles and V_{void} is the volume of voids.

Assuming (i) that microspheres assemble in the most common types of packing structure, i.e., a hexagonal close-packed (hcp) or a face-centered cubic (fcc) lattice, and (ii) that no particle deformation occurs when they come in contact, we obtain the particle fraction in a close-packed structure[14]

$$\phi = \pi\sqrt{2}/6 \approx 0.74 \quad (2)$$

Equation 2 implies that, to fill voids between particles upon annealing, the volume of shells, V_s, has to exceed at least $0.35V_{part.}$, i.e.,

$$V_s > 0.35V_{part} \quad (3)$$

For the core−shell microspheres shown in Figure 4c

$$V_{part} = {}^4/_3\pi(r_c + l_s)^3 \quad (4)$$

$$V_s = V_{part} - V_c = {}^4/_3\pi[(r_c + l_s)^3 - r_c^3] \quad (5)$$

where V_c is the volume of a core.

By substituting the expressions for V_s and V_c from (4) and (5) into (2), the minimum shell thickness required to fill interparticle voids was estimated to be $\sim 0.15r_c$. In reality, the reduction in the interparticle separation upon film formation has to be taken into account.[14] Thus, the thickness of shells that provides filling of voids and leaves a spacing between "core" particles has to be at least $0.2r_c$. The concentration of the core-forming polymer in the composite material for different volume ratios of the CFP and the SFP is given in Table 3. The italicized values correspond to the ratio between the core and shell dimensions that does not satisfy the requirement of $l_s \geq 0.2r_c$.

For the particle dimensions varying from 50 nm to 3 μm and the ratio between the core radius and the shell

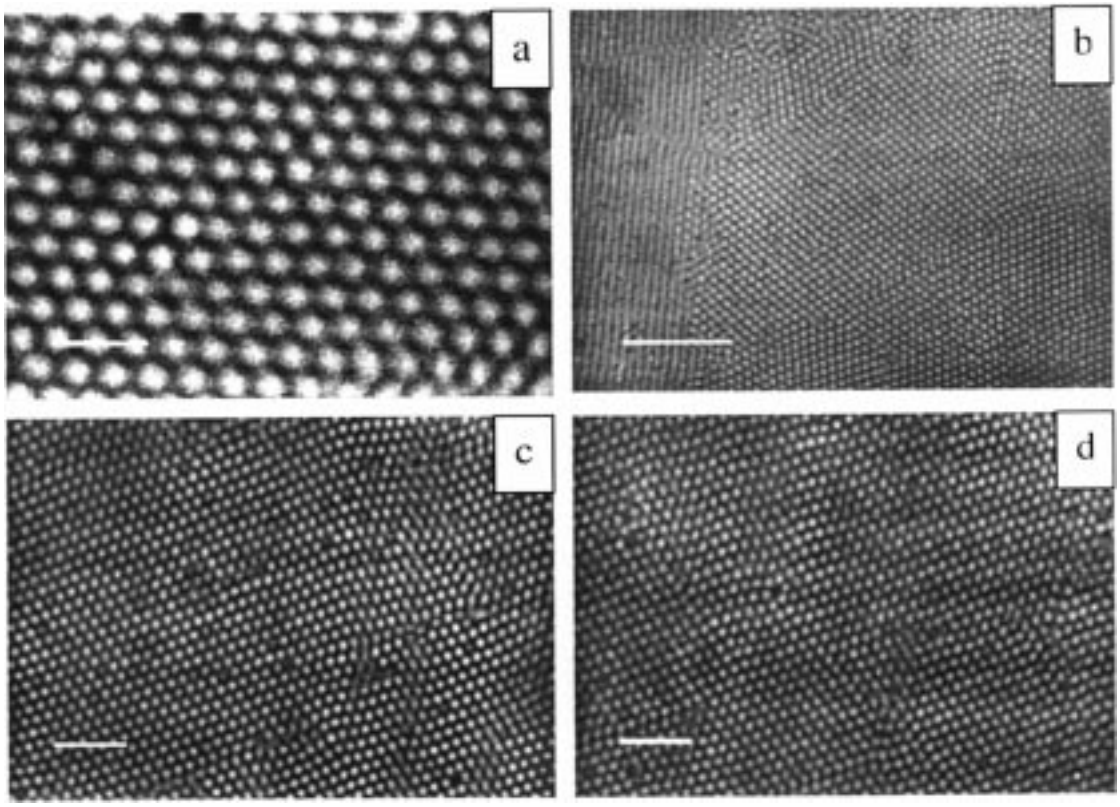

Figure 6. Confocal fluorescent microscopy images of the surface and bulk morphologies of the polymer nanocomposite obtained from core−shell latex particles with the core diameter of 650 nm and the shell thickness of 205 nm. Dye-labeled cores remain intact during annealing and appear as bright fluorescent spots on the background formed by inert shells. (a, b) Polymer morphology at the surface of the sample at different magnification. Polymer bulk morphology: (c) 30 μm below the surface; (d) 100 μm below the surface. Scale bar: (a) 2 μm; (b−d) 10 μm.

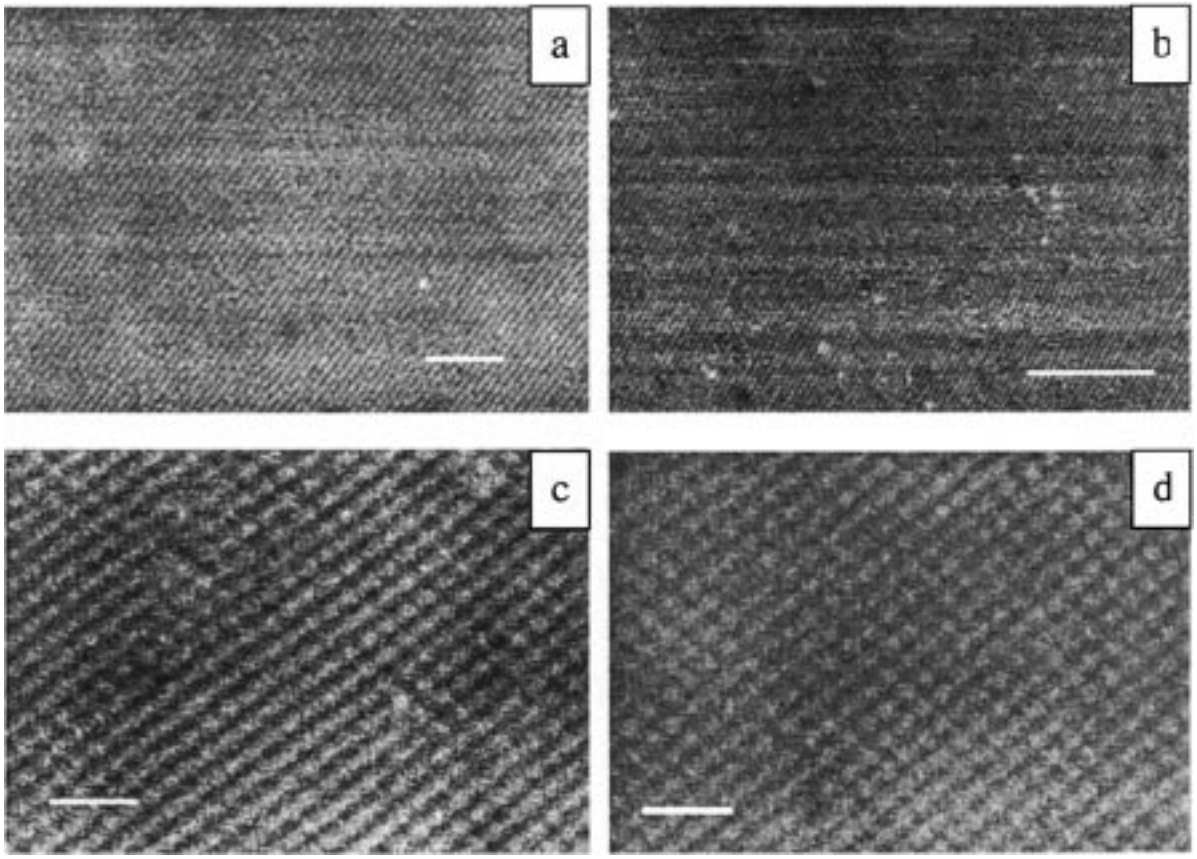

Figure 7. Confocal fluorescent microscopy images of the surface and bulk morphologies of the polymer material obtained from core−shell latex particles with the core diameter of 370 nm and the shell thickness of 95 nm: (a, b) polymer composite structure at the surface of the sample at different magnifications; polymer bulk structure (c) 15 μm below the surface (d) 50 μm below the surface. Scale bar: (a) 5 μm; (b) 10 μm; (c, d) 2 μm.

thickness $r_c/l_s = 0.2$, the number density of the "core" particles in the nanocomposite varies from 10^{11} to 10^{16} cm^{-3}, respectively.

Packing of Latex Particles. Assembly of latex particles in ordered arrays is a challenge at the forefront of material science.[1,3,10] In our work, formation of the ordered polymer nanocomposite was predetermined by ordering of the core−shell latex particles at the stage of their sedimentation. The method employed for the formation of large-scale defect-free arrays from concentrated latex dispersions is an issue of a different publication.[15] Here we discuss factors that influence particle organization from relatively dilute (1−10 wt %) dispersions.

Crystallization of settling latex particles was resolved from irridiscence of sediments. After water was carefully removed from the system, the irridiscence was observed at the surface of dry sediments. Ususally, after annealing such samples featured a large extent of ordering.

Crystallization of colloid silica particles from settling organophilic suspensions was thoroughly studied by Russel et al.[16] In our work, qualitative features of sedimenting latex microbeads were very similar to those observed in silica dispersions, although latex particles carried substantial surface charge. In the absence of external forces (excluding gravity), the regularity of particle packing was affected by their polydispersity, dimensions, volume fraction, and interparticle interactions. It was important that at the stage of sedimentation every particle settles as an individual unit. Increased electrostatic repulsion between particles and the dilution of the dispersion enhanced ordered packing.

Similar to settling silica particles,[16] packing of large and small latex microbeads gave different results. For large microspheres with the diameter 1050 nm, good ordering was achieved when particles settled from dilute dispersions. Particle sedimentation from dispersions with a solid content higher than ca. 2 wt % led to the coexistence of areas with a different crystalline order. Sedimentation of 560 nm core−shell latex particles provided good ordering within a wide range of latex concentrations varying from 1 to 10 wt %.

Any polydispersity in particle dimensions, e.g., caused by secondary seeding, led to a disrupted ordering. Small secondary particles caused distortions and defects in the structure of the nanocomposite polymer, even when their dimensions matched the sizes of voids between larger particles. Therefore, precise control of the dimensions of the particle cores and the particle shells was required at the synthetic stage.

The morphology of the material at both interfaces was influenced by the surface effects. Particle ordering was complicated when the roughness of the substrate was comparable to or exceeded the dimensions of settling microspheres. To reduce the number of defects at the film−substrate interface, an atomically smooth hydrophobized mica was used. The morphology of the air−film interface was influenced by the competition between the rate of water evaporation and the rate of particle sedimentation. To achieve better particle ordering, water evaporation was suppressed.

Morphology of the Composite Material. Atomic force microscopy (AFM) was used to study the surface structure of the composite material and to ensure the

absence of voids in it. Figure 5 displays the surface morphology of the polymer film formed by annealing of closely packed core−shell particles with the diameter 1050 nm. Highly ordered rigid "core" particles are embedded in a regular fashion in the matrix formed by the BMA−MMA copolymer. The dimensions of "core" particles compare well with those measured with SEM after the second stage of synthesis. No voids were observed in films in the experimental range of the dimensions of cores and shells.

The surface and the bulk morphologies of the polymer composite material were studied using laser confocal fluorescent microscopy. Imaging of the structure of 2D planes with a scanning step varying from 1 to 10 μm was carried out from the surface to ca. 200 μm in depth of the polymer material. A three-dimensional reconstruction of the 2D images enabled us to examine the bulk structure of the material. Figure 6 shows the morphology of the polymer composite prepared from latex microspheres composed of 640 nm cores and 205 nm thick shells. Rigid "core" particles are organized in a highly ordered array on the length scales varying from 40 to 80 μm in the $x-y$ plane and to more than 200 μm in the z-direction. In larger lateral planes, areas with a different symmetry divided by grain boundaries are sometimes observed as shown in Figure 6b. Ordering in a vertical direction was always retained to a greater extent. The surface morphology of the composite material at the air−film interface sometimes showed imperfections, which were rapidly "healed" at the remoteness from the surface of ca. 5−10 μm. Beyond this distance, polymer material possessed a regular bulk structure shown in Figure 6c,d.

Polymer material formed from core−shell latex particles with the diameter 560 nm featured more organized morphology shown in Figure 7. Although in this image the dimensions of latex cores and shells are almost at the verge of the lateral resolution of the confocal microscope, a highly periodic distribution of "core" microbeads can be resolved on the surface and in the bulk of the nanocomposite polymer material.

In addition to organized structure, the images presented in Figures 6 and 7 demonstrate another important advantage of the proposed approach: regardless of the extent of ordering, the "core" particles never aggregate, always being separated by a shell barrier.

Summary

The described method is a general approach for the development of polymer nanocomposites comprised of functionalized particles densely and regularly embedded in a polymer matrix. By using different combinations of the CFP and the SFP or by incorporating different functional groups in the CFP and the SFP, various properties can be tailored to the ultimate polymer material.

Moreover, a combination of the inorganic cores with the polymeric shells would lead to composite materials with challenging properties. In particular, nanocomposites in which core- and shell-forming materials possess a sufficient difference in the refractive index can be used as materials for photonic applications.

In the polymer composite material described in the current work, the T_g of the CFP is higher than the T_g of the SFP. However, a cross-linking of the SFP only produces latex particles with rigid shells and soft cores. The CFP can be later dissolved with suitable solvents, thus transforming a composite material to a porous film with a regular and controlled distribution of pores.

The incorporation of various functionalities in either CFP or SFP opens new challenges. For example, an attachment of chromophores to the "core" particles can be used for producing polymer materials for 3D memory storage. In such material, every "core" particle would represent a single bit. Recently, a possibility of a permanent recording induced by a local photobleaching of NBD in "core" particles has been demonstrated by our group.[13]

Alternatively, electroconductive or magnetic properties can be tailored to either the "core" particles or the matrix polymer using an attachment of the corresponding species to the CFP or the SFP.

Acknowledgment. The authors thank Xerox Research Centre of Canada and NSERC Canada for financial support of this work. The authors are grateful to Prof. M. A. Winnik and Dr. Jaan Noolandi for helpful discussions. We also thank Dr. S. Sosnowski for his help in the synthesis of NBD dye.

References and Notes

(1) Wijnhoven, J. E. G. J.; Vos, W. L. *Science* **1998**, *281*, 802.
(2) Tsukruk, V. V. *Prog. Polym. Sci.* **1997**, *22*, 247.
(3) Tse, A. S.; Wu, Zh.; Asher, S. A. *Macromolecules* **1995**, *28*, 6533.
(4) Micheletto, R.; Fukuda, H.; Ohtsu, M. *Langmuir* **1995**, *11*, 3333.
(5) Holland, B. T.; Blanford, C. F.; Stein, A. *Science* **1998**, *281*, 538.
(6) Kim, E.; Xia, Y.; Whitesides, G. M. *Adv. Mater.* **1996**, *8*, 245.
(7) Feng, J.; Winnik, M. A.; Shivers, R. R.; Clubb, B. *Macromolecules* **1995**, *28*, 7671.
(8) Chevalier, Y.; Hidalgo, M.; Cavaille, J.-Y.; Cabane, B. Small-Angle Neutron Scattering Studies of Composite Latex Film Structure. In *ACS Symp. Ser.* **1996**, *648*, 245.
(9) Li, L.; Sosnowski, S.; Kumacheva, E.; Winnik, M. A. *Langmuir* **1996**, *12*, 2141.
(10) (a) Asher, S. A.; Holtz, J.; Liu, L.; Wu, Z. *J. Am. Chem. Soc.* **1994**, *116*, 4997. (b) Sunkara, H. B.; Weissman, J. M.; Penn, B. G.; Frazier, D. O.; Asher, S. A. *Polym. Prepr.* **1996**, *39*, 453.
(11) O'Callagham, K. Y.; Paine, A. Y.; Rudin, A. *J. Appl. Polym. Sci.* **1995**, *58*, 2047. O'Callagham, K. Y.; Paine, A. Y.; Rudin, A. *J. Polym. Sci., Part A: Polym. Chem.* **1995**, *33*, 1849.
(12) Sosnowski, S.; Feng, J.; Winnik, M. A. *J. Polym. Sci., Polym. Chem.* **1994**, *32*, 1497.
(13) Mayoral, R.; Requena, J.; Moya, J. S.; Lopez, C.; Cintas, A.; Miguez, H.; Moseguer, F.; Vazquez, L.; Holdago, M.; Blanco, A. *Adv. Mater.* **1997,** *9*, 257.
(14) Meyer, E. F. III. Geometric Considerations in Latex Film Formation. In *ACS Symp.* Ser. **1996**, *648*, 44.
(15) Vickreva, O.; Kalinina, O.; Kumacheva, E., to be published.
(16) Davis, K. E.; Russel, W. B.; Glantschnig, W. J. *J. Chem. Soc., Faraday Trans.* **1991**, *87*, 411.
(17) Kalinina, O.; Kumacheva, E.; Lilge, L. *Adv. Mater.* **1999**, *11*, 231.

MA981583O